

## SEYFERT GALAXY NARROW-LINE REGIONS. I. OBSERVATIONS OF [O III] $\lambda 5007^1$

J. M. VRTILEK

Harvard-Smithsonian Center for Astrophysics, and NASA/Goddard Institute for Space Studies

AND

N. P. CARLETON

Harvard-Smithsonian Center for Astrophysics

Received 1984 October 19; accepted 1985 January 16

### ABSTRACT

High-resolution ( $23 \text{ km s}^{-1}$ ) spectra of the [O III] emission line at 500.7 nm from the nuclear regions of 32 Seyfert galaxies and low-redshift QSOs have been obtained at the Smithsonian Institution/University of Arizona Multiple Mirror Telescope. The properties of the data are summarized by a group of measures which efficiently describe the entire line profiles, are stable in the presence of noise, and have easily visualized geometric meaning.

The distributions of line profile measures are shown. In particular, typical [O III] FWHM values of 200–520  $\text{km s}^{-1}$  (mean  $\pm 1 \sigma$ ) and a highly significant tendency for the lines to fall off more slowly on the blue than on the red side of the peak have been found, in agreement with previous work. Using galaxian system velocities obtained from absorption-line measurements, the distribution of differences between [O III] emission-line velocities and galaxian system velocities has been determined; in disagreement with previous work, this distribution has been found to be consistent with symmetry about zero difference velocity.

*Subject headings:* galaxies: nuclei — galaxies: Seyfert — line profiles

### I. INTRODUCTION

From the earliest investigations, emission-line spectra have served both to identify and define active galaxies and also to diagnose the physical conditions in the regions emitting the lines. The current standard picture of active galaxies calls for a highly compact nonthermal source surrounded by a subparsec broad-line region and a more extended narrow-line region. Temperatures, densities, column densities, and to some extent even abundances in these regions have been studied (e.g., Halpern 1982; Ferland and Mushotzky 1982; Kwan and Krolik 1981; Davidson and Netzer 1979, and references therein). There is some understanding of the interaction of central source ionizing radiation with the line-emitting material, and also a rough geometric picture of this material distributed in clouds of low filling factor probably immersed in a thin, hot medium (Krolik and Vrtilek 1984; Krolik, McKee, and Tarter 1981).

Many questions, however, are left unanswered in this picture. Among them are the following: What are the sources and sinks for this material? What relationship, if any, is there between the material of the narrow-line and broad-line regions? How are the material motions related—if at all—to the feeding of a central engine and to the (unknown) duration of galaxian activity?

High-resolution spectroscopy of the emission lines offers an approach to this problem. The line widths of even the narrowest emission lines observed in active galaxies are far in excess of the thermal widths at the relevant temperatures. It is generally accepted that the cause is dynamical: mass motions are large compared to thermal motions. This means that the emission-line profiles encode information on the velocity distributions of the material that produced them. Until recently, the com-

bination of large light collecting area and efficient detectors required for high signal-to-noise and high resolution observations of active galaxies was not available; as a result, the detailed structure of the emission lines has received only limited attention (e.g., Phillips *et al.* 1983; Heckman *et al.* 1981; Pelat, Alloin, and Fosbury 1981).

The purpose of the present work is the investigation of active galaxy narrow-line region (NLR) kinematics based on spectra of the [O III]  $\lambda 5007$  emission line—generally the brightest optically accessible narrow line for low-redshift objects—from 32 active galactic nuclei. In this paper, a method of approximate description for the emission lines in terms of a small number of numerical measures is developed. These are used to examine the distribution of line characteristics and to search for relationships between properties of the lines and other properties of the active galaxies. In a subsequent paper (Vrtilek 1985, hereafter Paper II), we compare systematically a class of simple models to the data in an attempt to clarify what classes of motion are or are not allowed.

### II. OBSERVATIONS

The high-resolution spectroscopic data presented here were obtained with the echelle spectrograph at the Multiple Mirror Telescope (MMT) in a series of runs from 1980 June to 1981 October. In the configuration used for these observations, the echelle spectrograph was preceded by an image stacker and reimaging lens (Chaffee and Latham 1982); the slit size used (200  $\mu\text{m}$ ) then corresponds to a  $2''.2 \times 2''.2$  square on the sky and determines the spectral resolution of  $23 \text{ km s}^{-1}$  or  $0.4 \text{ \AA}$  at [O III]  $\lambda 5007$ . The resolution was chosen to be comparable to the narrowest features which could be emitted in principle while avoiding excessive light losses at the slit. The detector used was a (one-dimensional) intensified Reticon system (Latham 1982; Davis and Latham 1979). Because of the close spacing of the echelle orders and the presence of the image

<sup>1</sup> Research reported here used the Multiple Mirror Telescope, a joint facility of the Smithsonian Institution and the University of Arizona.

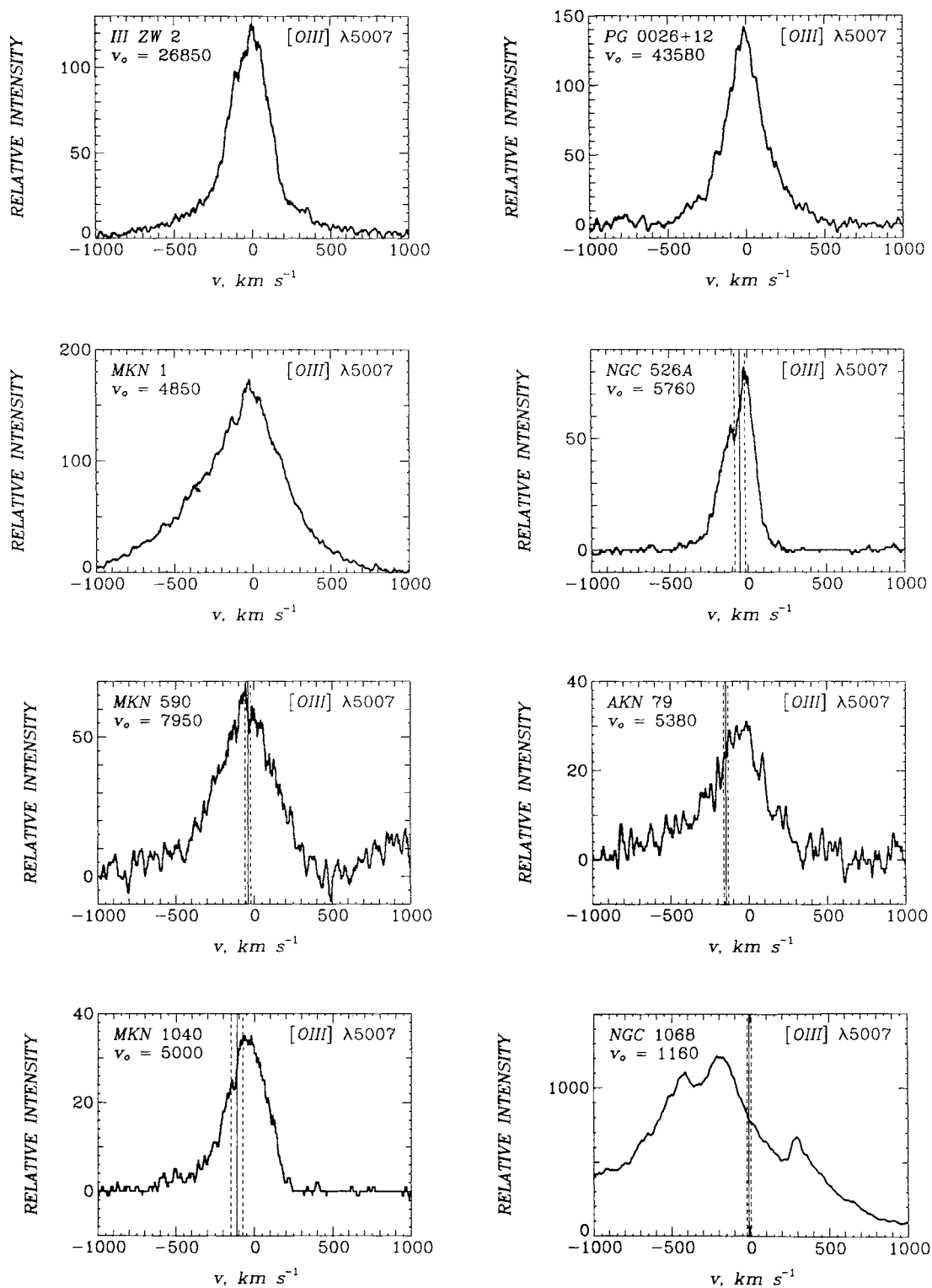


FIG. 1.— $[O III] \lambda 5007$  emission lines from the nuclear regions of eight Seyfert galaxies and QSOs. A linear baseline has been removed. The spectra were obtained at a resolution of  $23 \text{ km s}^{-1}$  with a  $2'' \times 2''$  slit. A  $2000 \text{ km s}^{-1}$  segment of spectrum is shown;  $v_0$  is the heliocentric velocity ( $cz$ ) in kilometers per second at spectrum center. Positive velocities are to the red and negative to the blue. The ordinate units indicate the approximate number of photon counts per pixel near the center of the spectrum. Vertical lines indicate galaxy system velocities (with dotted lines giving  $\sim 1 \sigma$  errors) as determined from low-resolution spectra. This is described in detail in § IV.

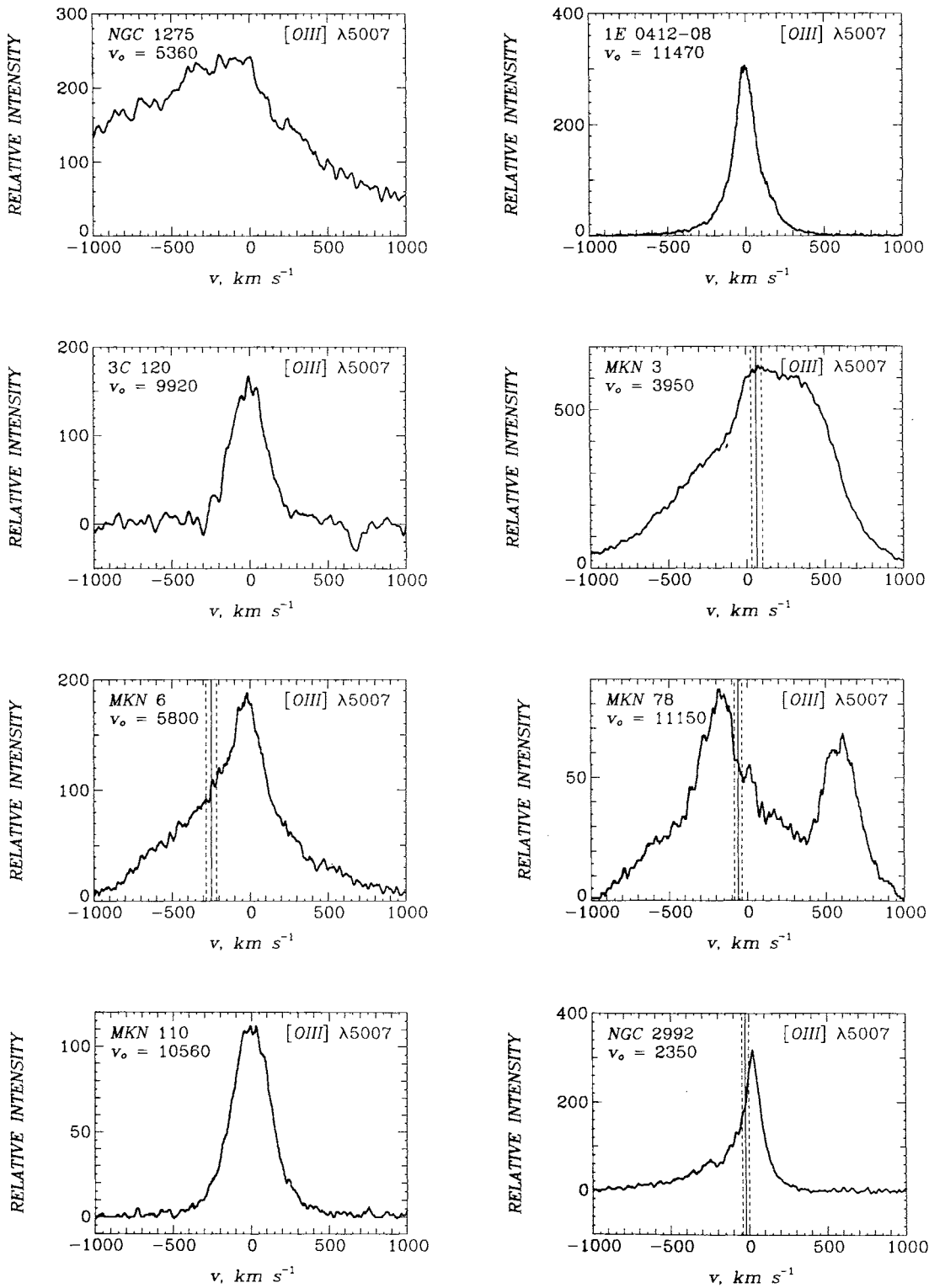


FIG. 2.—Same as for Fig. 1

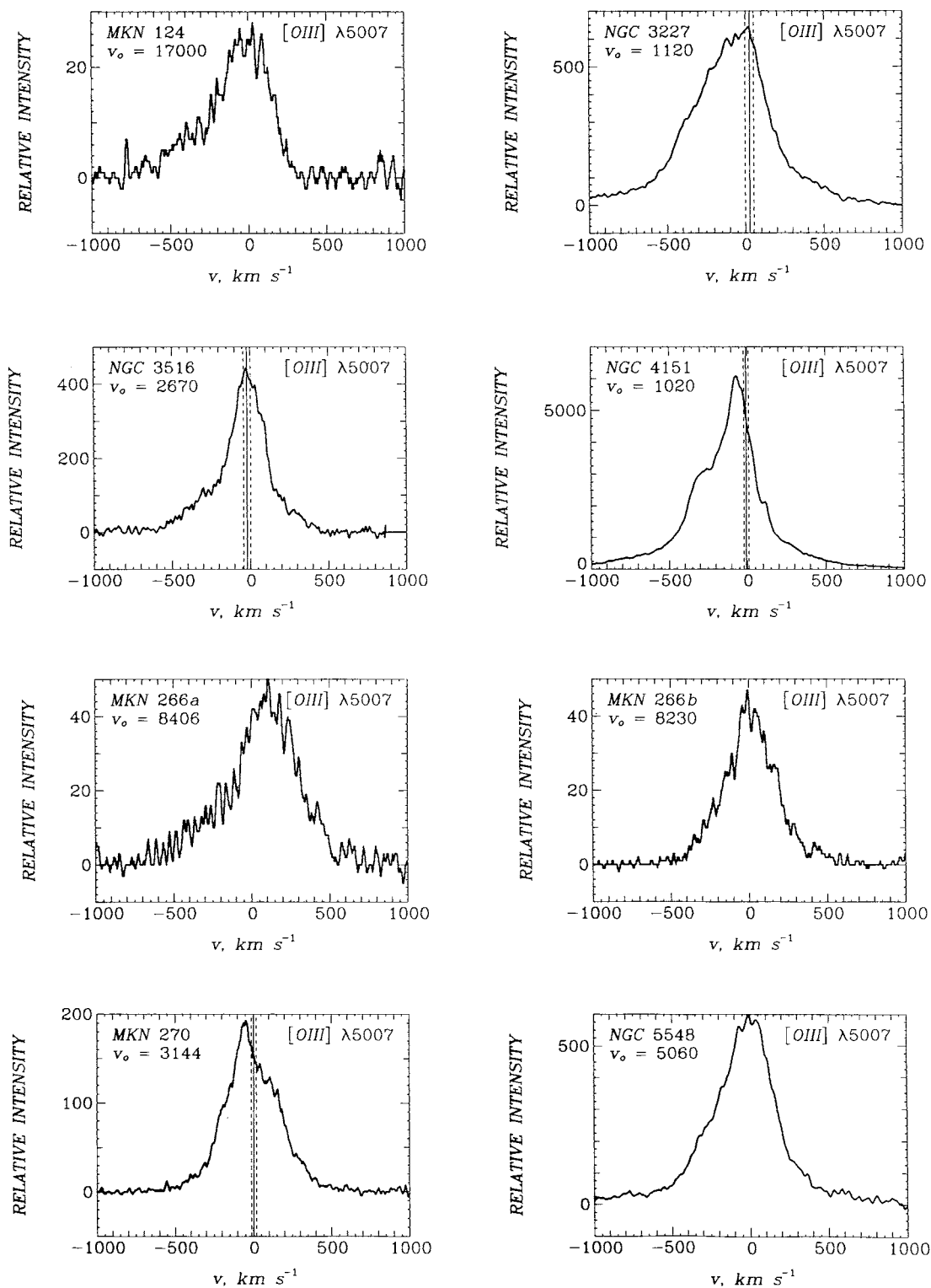


FIG. 3.—Same as for Fig. 1

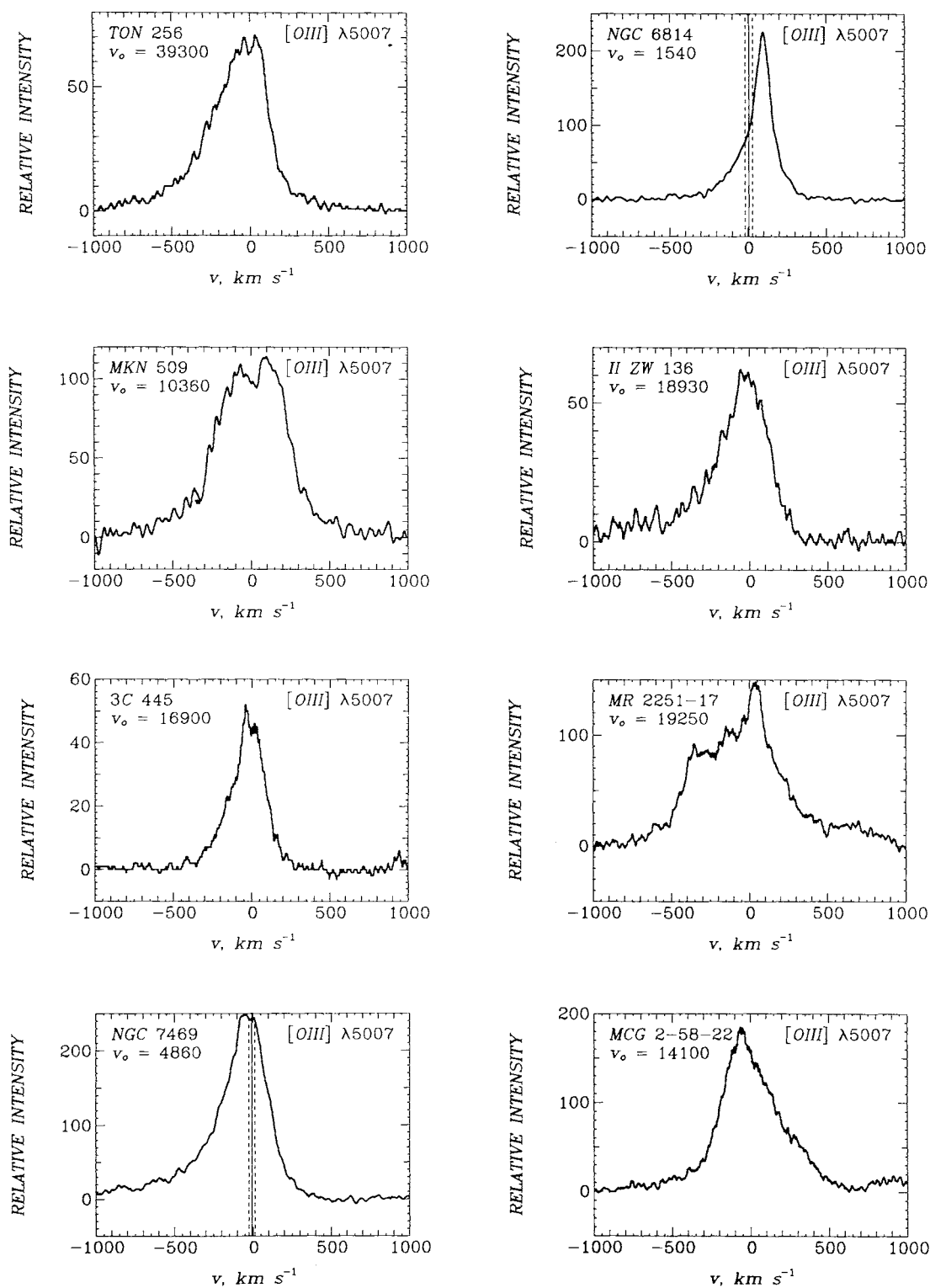


FIG. 4.—Same as for Fig. 1

stacker optics, simultaneous sky subtraction using the second Reticon row was not possible. Depending on the image tube configuration,  $\sim 35\text{--}50 \text{ \AA}$  of spectrum were covered at once. The telescope/spectrograph/detector combination achieved a counting efficiency of  $\sim 1\%$ .

The reduction of the raw data to a relative intensity versus velocity scale involved several major steps:

1. The nonuniform image tube response, the wavelength-dependent echelle efficiency, and the detector fixed pattern were removed through division by incandescent lamp exposures. A minor consequence of this process is that count levels across the spectrum are not exactly preserved.

2. Lines in (thorium-argon) lamp exposures obtained immediately before and after each object exposure were identified, and a seventh-order polynomial dispersion solution was obtained. Errors in the wavelength fit are typically under  $0.1 \text{ \AA}$  ( $6 \text{ km s}^{-1}$ ) and hence are negligible for any subsequent purpose here.

3. The spectra were converted from a wavelength scale to a heliocentric velocity scale and smoothed to the instrumental resolution.

4. A linear baseline (including galaxy continuum, sky background, and [usually negligible] detector dark counts) was removed from each of the spectra. Lack of knowledge of the true continuum position implies that no algorithm can be developed to remove correctly and objectively the baseline; here the baseline position was estimated by eye.

In Figures 1 to 4 the reduced data are presented in graphical form. The zero level corresponds to the baselines assigned by eye. The heliocentric velocity ( $cz$  in  $\text{km s}^{-1}$ ) corresponding to the zero of the velocity axis is given as  $v_0$  on each of the plots.

The collection of 32 objects observed here does not constitute a representative or complete sample of active galaxies. They were chosen to cover a wide range in intrinsic luminosity, in galaxy axial ratio, and in type (Weedman 1977), and in class (Steiner 1981). In addition, ready accessibility to observation from a latitude of  $32^\circ \text{ N}$  and relatively high apparent brightness ( $m_v \leq 16$ ) were required characteristics. This is a small subset of currently known Seyferts, which number  $\sim 300$  (Huchra 1983).

A log of the observations is shown in Table 1. The total integration time is 21.3 hr divided among 13 nights. Table 1 shows also an approximate signal-to-noise indicator. Since the S/N ratio varies across each spectrum and since the noise characteristics are not entirely Poisson, it is not possible to assign precise signal-to-noise ratios to the profiles. Nonetheless, it may be useful to have indicator of the quality of the spectra. The ratio we give was computed as the quotient of the peak value and the mean of the rms fluctuations in the bluest and redmost 10% of each spectrum.

### III. CHARACTERISTICS OF SEYFERT [O III] LINES

#### a) Method of Emission-Line Description

This section presents a quantitative method for describing the observed line profiles. We use a set of seven dimensionless measures to describe the line profile shape and one measure, the FWHM (denoted W50 here), with dimensions of velocity to fix the scale. Five of the seven dimensionless measures, defined in terms of the velocity positions at 20%, 50%, and 80% of the peak height, describe the profiles above the 20% of peak level, and the other two characterize the wings below the 20% level. Two of the measures are the scaled full line widths at the 80%

(W80/W50) and 20% (W20/W50) levels. The line asymmetries are described by the (scaled) shifts of the line centers at the 80% (C80/W50), 50% (C50/W50), and 20% (C20/W20) levels from the line peak position; line center shifts to the red (blue) are given as positive (negative). An extension of this approach is not suitable for profile description below the 20% level for several reasons: the wings are strongly curved, so that joining a few points by line segments is not a good representation; the flatness of the profile wings implies that even small baseline uncertainties cause large errors in locating crossings at a specified fraction of the peak height; and determining crossing points at one or two additional levels would not give a sense of the smooth approach to the baseline found in the data. Accordingly, a different approach has been taken. The essential feature to be described is the scale of drop-off of the wings. Inspection of the data suggested fitting the function  $A + B \exp(-v/C)$  below the 20% level; the parameter of interest is  $C$ . This e-folding scale, designated CB (CR) for the blue (red) wing, determined by a least-squares fit, leads to two wing measures: CB/W50 and CR/W50. The computation of the profile measures is illustrated in Figure 5. Figures 6a–6c show the results of exponential fits to the wings of three data profiles; although no formal quality-of-fit analysis has been done, this function provides a visually excellent fit to the wings of all of the data.

There are two major sources of uncertainty in determining the line profile measures: noise due to observing only a limited number of photon events and uncertainty in baseline location. In the present data the more significant uncertainties arise, in general, from the baseline determination. This is a systematic problem: the location of the continuum for the [O III]  $\lambda$ 5007 line is complicated by the presence of [O III]  $\lambda$ 4959 toward the blue and of Fe II (in some sources) toward the red. In addition, the wavelength range of the available data is limited. These effects cannot be taken into account in a statistically rigorous fashion, but an estimate of the sensitivity of the measures to baseline changes was made by recomputing the line profile measures after shifting the baselines by the rms fluctuations computed from the extremes of each spectrum. A detailed justification and discussion of this procedure has been given by Vrtilek (1983).

Table 2 lists the W50 values and the heliocentric velocities of the peaks for the 32 data profiles; Table 3 lists the seven dimensionless line profile shape measures. The latter permit a rough reconstruction of the shape of an entire profile, and the former establish the width scale and the velocity position for it. These data are not spectrophotometric; hence, no amplitude scale is supplied. (Fluxes in the major optical emission lines from most of these sources have been published; see, e.g., the compilation of Steiner 1981.)

This method of quantitative line profile characterization was chosen after extensive trials of various approaches. It has several virtues: (1) The value of each measure fixes a single, easily visualized aspect of a profile. (2) The values of the measures are stable in the presence of baseline uncertainties and noise. The total spread among the data in each measure is typically  $\sim 10$  times the magnitude of the mean assigned error. (3) There are no redundant measures. Omission of any one leaves a clear gap in the information required for an approximate reconstruction of the profiles from the measures. No significant pairwise correlations remain between measures other than between C20/W50 and C50/W50, which mainly indicates that the sense of asymmetry in the profiles tends to be preserved between the 20% and 50% levels. (4) The measures

TABLE 1  
LOG OF OBSERVATIONS

| Object                              | UT Date Observed | Integration Time (minutes) | S/N <sup>a</sup> | $\alpha_{1950}^b$                                  | $\delta_{1950}^b$ | Type <sup>c</sup> | Class <sup>d</sup> |
|-------------------------------------|------------------|----------------------------|------------------|--|-------------------|-------------------|--------------------|
| 0008+10 III Zw 2 .....              | 1981 Oct 9       | 30                         | 109              | 00 <sup>h</sup> 07 <sup>m</sup> 56 <sup>s</sup> .7 | +10°41'48"        | 1                 | A2                 |
| 0026+12 PG .....                    | 1981 Oct 9       | 30                         | 57               | 00 26 38.1   | +12 59 30         | QSO               | A                  |
| 0113+32 Mrk 1 .....                 | 1981 Oct 8       | 30                         | 69               | 01 13 19.6   | +32 49 33         | 2                 | C                  |
| (NGC 449)                           |                  |                            |                  |  |                   |                   |                    |
| 0121-35 NGC 526A .....              | 1981 Oct 9       | 30                         | 89               | 01 21 37.3   | -35 19 32         | NELG              | B*                 |
| (MCG 6-4-19)                        |                  |                            |                  |  |                   |                   |                    |
| 0212-01 Mrk 590 .....               | 1981 Oct 8       | 30                         | 21               | 02 12 00.4   | -00 59 58         | 1                 | B                  |
| (NGC 863)                           |                  |                            |                  |  |                   |                   |                    |
| 0214+38 AKN 79 .....                | 1981 Oct 9       | 30                         | 14               | 02 14 19.8   | +38 10 59         | 1                 | A?*                |
| 0225+31 Mrk 1040 .....              | 1981 Oct 9       | 30                         | 61               | 02 25 14.5   | +31 05 23         | 1                 | B*                 |
| (NGC 931)                           |                  |                            |                  |  |                   |                   |                    |
| 0240-00 NGC 1068 .....              | 1980 Sep 28      | 10                         | °                | 02 40 07.1   | -00 13 31         | 2                 | C                  |
| 0316+41 NGC 1275 .....              | 1980 Nov 22      | 60                         | °                | 03 16 29.6   | +41 19 52         | ?                 | ?                  |
| 0412-08 1E .....                    | 1981 Oct 9       | 15                         | 490              | 04 12 27.0   | -08 03 08         | QSO               | B*                 |
| 0430+05 3C 120 .....                | 1980 Nov 22      | 60                         | 32               | 04 30 31.6   | +05 15 00         | 1/BLRG            | B                  |
| (II Zw 14)                          |                  |                            |                  |  |                   |                   |                    |
| 0609+71 Mrk 3 .....                 | 1981 Apr 21      | 30                         | 41               | 06 09 48.4   | +71 03 11         | 2                 | C                  |
| 0645+74 Mrk 6 .....                 | 1981 Oct 8       | 10                         | 59               | 06 45 43.9   | +74 29 10         | 1.5               | B                  |
| (IC 450)                            |                  |                            |                  |  |                   |                   |                    |
| 0737+65 Mrk 78 .....                | 1981 Oct 8       | 20                         | 23               | 07 37 56.8   | +65 17 42         | 2                 | C                  |
| 0921+52 Mrk 110 .....               | 1981 Oct 8       | 20                         | 125              | 09 21 44.4   | +52 30 08         | 1                 | B                  |
| 0943-14 NGC 2992 .....              | 1981 Apr 21      | 15                         | 116              | 09 43 17.6   | -14 05 45         | NELG              | B*                 |
| (Arp 245)                           | 1981 Apr 22      | 40                         |                  |  |                   |                   |                    |
| 0945+50 Mrk 124 .....               | 1981 Oct 8       | 30                         | 18               | 09 45 24.3   | +50 43 29         | 1                 | A1                 |
| 1020+20 NGC 3227 .....              | 1980 Nov 22      | 60                         | 141              | 10 20 46.8   | +20 07 06         | 1.2               | A2                 |
| 1103+72 NGC 3516 .....              | 1981 Apr 21      | 35                         | 77               | 11 03 22.8   | +72 50 20         | 1                 | A2                 |
|                                     | 1981 Apr 22      | 30                         |                  |  |                   |                   |                    |
| 1208+39 NGC 4151 <sup>f</sup> ..... | 1980 Apr 28      | 51                         | 165              | 12 08 01.1   | +39 41 02         | 1.5               | B                  |
|                                     | 1980 May 4       | 60                         |                  |  |                   |                   |                    |
| 1336+48 Mrk 266 <sup>a</sup> .....  | 1981 Jun 11      | 53                         | 24               | 13 36 14.7   | +48 31 53         | 2                 | C*                 |
| (NGC 5256)                          |                  |                            |                  |  |                   |                   |                    |
| (I Zw 67)                           |                  |                            |                  |  |                   |                   |                    |
| Mrk 266b .....                      | 1981 Jun 11      | 30                         | 61               |  |                   | 2                 | C*                 |
| 1339+67 Mrk 270 .....               | 1981 Jun 11      | 30                         | 86               | 13 39 41.4   | +67 55 27         | 2                 | C                  |
| (NGC 5283)                          |                  |                            |                  |  |                   |                   |                    |
| 1415+25 NGC 5548 .....              | 1980 Jun 24      | 60                         | 77               | 14 15 43.5   | +25 22 01         | 1.5               | A2                 |
| 1612+26 Ton 256 .....               | 1981 Oct 9       | 15                         | 66               | 16 12 09.0   | +26 12 14         | QSO               | B?                 |
| 1939-10 NGC 6814 .....              | 1980 Jun 19      | 30                         | 134              | 19 39 55.8   | -10 26 33         | 1                 | A*                 |
|                                     | 1980 Jun 24      | 48                         |                  |  |                   |                   |                    |
|                                     | 1981 Jun 11      | 30                         |                  |  |                   |                   |                    |
| 2041-10 Mrk 509 .....               | 1980 Jun 28      | 24                         | 30               | 20 41 26.3   | -10 54 18         | 1                 | B                  |
| 2130+09 II Zw 136 .....             | 1981 Oct 8       | 30                         | 33               | 21 30 01.2   | +09 55 01         | 1                 | A1                 |
| (PG 2130+09)                        | 1981 Oct 8       | 30                         |                  |  |                   |                   |                    |
| 2221-02 3C 445 .....                | 1981 Oct 9       | 30                         | 45               | 22 21 14.7   | -02 21 27         | BLRG              | B                  |
| 2251-17 MR .....                    | 1981 Oct 8       | 30                         | 42               | 22 51 25.9   | -17 50 54         | QSO               | B                  |
| 2300+08 NGC 7469 .....              | 1980 Jun 26      | 23                         | 93               | 23 00 44.4   | +08 36 16         | 1                 | A1                 |
|                                     | 1980 Nov 22      | 30                         |                  |  |                   |                   |                    |
| 2302-08 MCG 2-58-22 .....           | 1981 Oct 8       | 30                         | 80               | 23 02 07.2   | -08 57 19         | 1                 | B                  |

<sup>a</sup> S/N estimated as the peak value divided by the average of the rms fluctuations of the bluest and reddest 10% of each spectrum.

<sup>b</sup> References for object coordinates are Burbidge, Crowne, and Smith 1977; Burbidge and Crowne 1979; Clements 1981; Gallouet, Heidmann, and Dampierre 1975; Hewitt and Burbidge 1980; Kojoian, Elliott, and Tovmassian 1978; Nieto 1978; Peterson 1973; Steiner, Grindlay, and Maccacaro 1982; Wilson and Meurs 1978.

<sup>c</sup> References for object type area Markarian, Lipovetskii, and Stepanyan 1977; Mushotzky 1982; Osterbrock 1977; Osterbrock and Koski 1976; Petrosian 1980; Phillips 1980; Puetter *et al.* 1981; Steiner, Grindlay, and Maccacaro 1982; Ward *et al.* 1978; Weedman 1977; Yee and Oke 1978.

<sup>d</sup> The class is as given by Steiner 1981, except as indicated by asterisk (\*), where determinations have been made in the course of this work.

<sup>e</sup> Line too wide; no baseline available.

<sup>f</sup> Indicates data obtained at Whipple Observatory 1.5 m telescope (NGC 4151 only); all other data obtained at MMT.

<sup>g</sup> Mrk 266a and b are associated objects separated by 12"; "a" refers to the NE and "b" to the SW nucleus (Petrosian, Saakyan, and Khachikyan 1980).

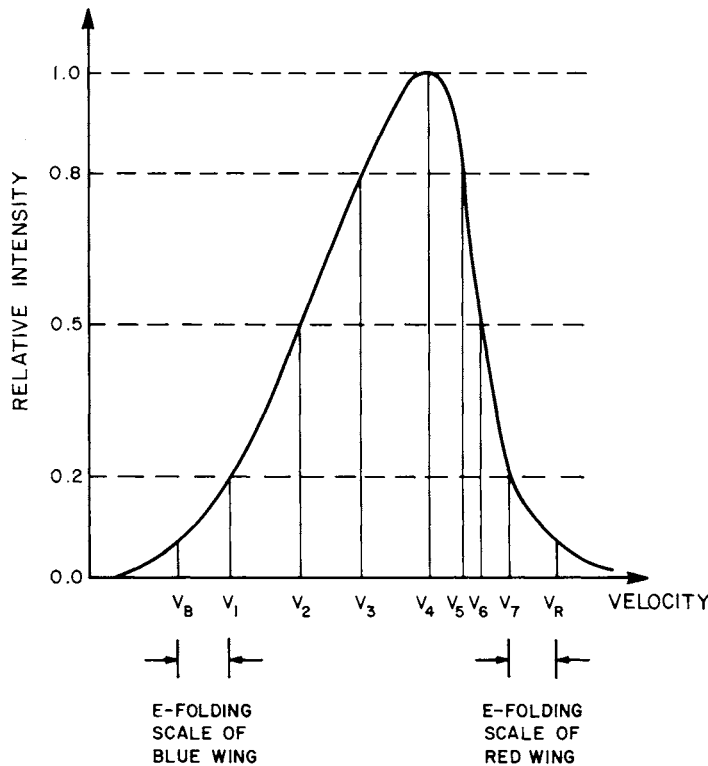


FIG. 5.—Schematic illustration of computation of line profile measures:  $W80 = V5 - V3$ ;  $W50 = V6 - V2$ ;  $W20 = V7 - V1$ ;  $C80 = [(V3 + V5)/2] - V4$ ;  $C50 = [(V2 + V6)/2] - V4$ ;  $C20 = [(V1 + V7)/2] - V4$ ;  $CB = V1 - V_B$ ;  $CR = V_R - V7$ .

describe the data with sufficient completeness to discriminate between any substantially different cases. At least for relatively smooth, unimodal profiles, only minor differences across short sections can exist between two profiles without effecting a change in at least one of the measures.

Narrow-line [O III] data similar to those presented here, although of lower resolution, have been obtained by Heckman *et al.* (1981, hereafter HMVB) and by Heckman, Miley, and Green (1984) in the only published studies of extent comparable to the present work. A reasonably detailed comparison is possible. The method of characterization used by HMVB for their data differs somewhat from that presented here: there is no description of the lines below the 20% of peak level, and the reference point for line asymmetry measurement is the line center at half-maximum rather than the peak. Their measures can be derived from those used in this work (although the reverse is not possible); the conversion is given in Table 4.

Of the galaxies where observations are available in common, five (Mrk 3, NGC 3227, Mrk 270, NGC 5548, and NGC 7469) have measures in good agreement. (The  $W80$  values for Mrk 270 and NGC 7469 are discrepant, but in a direction which can be explained by the coarser resolution of the measurements of HMVB.) 3C 120 shows a somewhat more asymmetric and more strongly peaked profile in the data of Heckman, Miley, and Green (1984) than in the present work. Three galaxies (Mrk 6, NGC 2992, and NGC 4151) show systematically larger widths at all levels and substantially more symmetric profiles in the data of HMVB than in the present data. These objects have narrow-line regions which are extended on a scale of several arc seconds, and slit size effects are probably important.

#### b) Distribution of Data Properties

The distributions of the data in the line profile measures described in the previous section are shown in Figures 7a-7h. The three objects whose NLRs have probably been under-sampled by the slit (Mrk 6, NGC 2992, and NGC 4151) are shown as dashed extensions to the histograms. As indicated previously, the objects represented in these distributions are not a true random sample of Seyfert galaxies. The sample is quite strongly flux-limited, as may be expected from the joint requirements that the objects in it span a large range in intrinsic luminosity and have high apparent brightness. As a consequence, the projected slit sizes at the objects are correlated with the object luminosity. Accordingly, the possible existence of correlations between the narrow-line properties and the projected slit extent has been examined; none were found.

In spite of the nonrepresentative nature of the sample, several interesting points may be made about the distributions of [O III] line characteristics: (1) Typical FWHM values are  $\sim 200-520 \text{ km s}^{-1}$  (mean  $\pm 1 \sigma$ ); the total measured range is much larger, from 129 to 904  $\text{km s}^{-1}$ . These measurements discriminate against the very widest lines (such as from NGC 1068 or NGC 1275) which cannot be included here due to limited spectral coverage; these seem to arise primarily in occasional peculiar Seyfert 2 galaxies. These results are in good general agreement with the lower resolution line width measurements of HMVB and of Feldman *et al.* (1982). (2) Using  $C20/W50$  as a good overall measure of line asymmetry, it is evident that there is a pronounced tendency in the data for negative asymmetry (i.e., slower falloff on the blue than on the

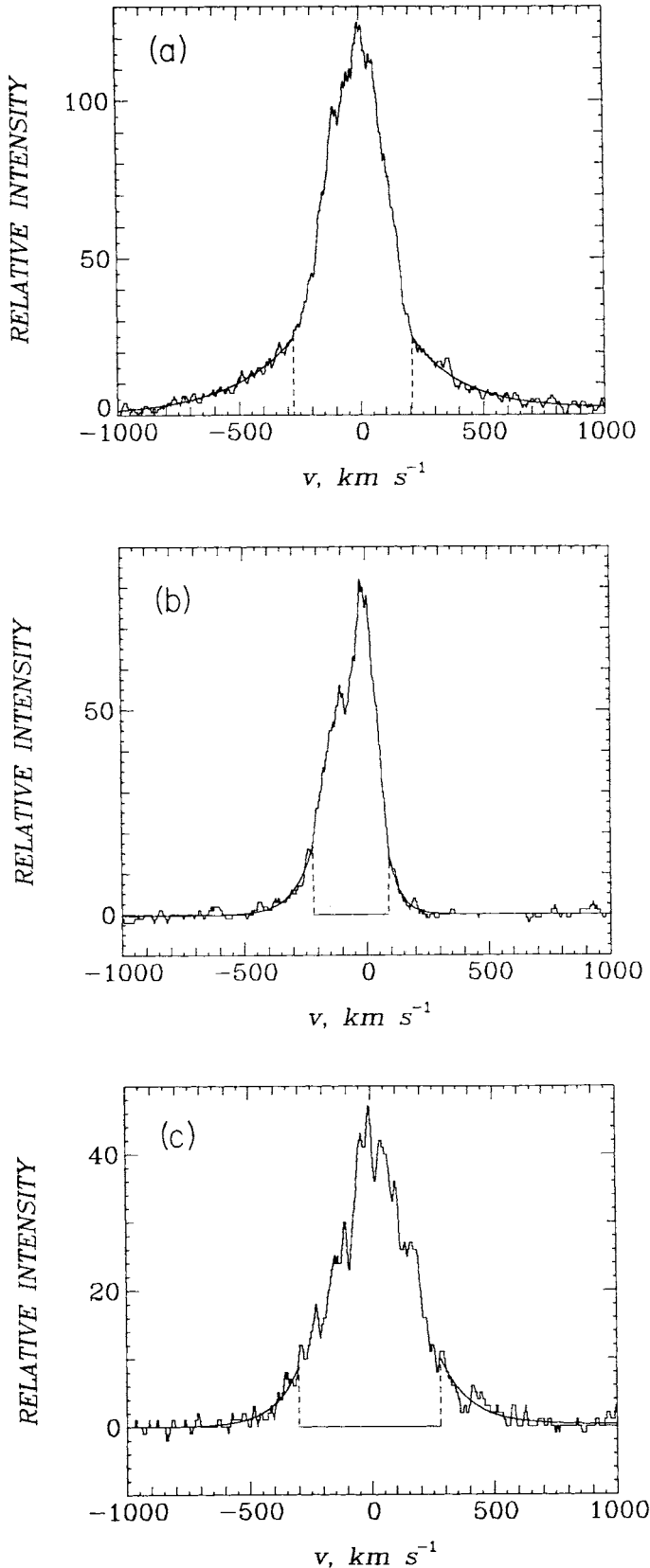


FIG. 6.—Examples of exponential functions fitted (in a least-squares sense) to the wings (i.e., below 20% of peak) of three data profiles: (a) III Zw 2, (b) NGC 526A, and (c) Mrk 266b.

TABLE 2  
FWHM (W50) AND HELIOCENTRIC PEAK VELOCITY  
VALUES FOR [O III] EMISSION LINES

| Object              | W50<br>( $\text{km s}^{-1}$ ) | Heliocentric Velocity<br>( $cz$ ) of Line Peak <sup>a</sup><br>( $\text{km s}^{-1}$ ) |
|---------------------|-------------------------------|---|
| 0008+10 III Zw 2    | $307 \pm 5$                   | 26850   |
| 0026+12 PG          | $247 \pm 8$                   | 43565   |
| 0113+32 Mrk 1       | $521 \pm 28$                  | 4820  |
| 0121-35 NGC 526A    | $210 \pm 5$                   | 5740  |
| 0212-01 Mrk 590     | $397 \pm 22$                  | 7890  |
| 0214+38 AKN 79      | $354 \pm 34$                  | 5370  |
| 0225+31 Mrk 1040    | $304 \pm 10$                  | 4945  |
| 0240-00 NGC 1068    | <sup>b</sup>                  | <sup>b</sup>  |
| 0316+41 NGC 1275    | <sup>b</sup>                  | <sup>b</sup>  |
| 0412-08 1E          | $160 \pm 5$                   | 11455   |
| 0430+05 3C 120      | $270 \pm 17$                  | 9920  |
| 0609+71 Mrk 3       | $904 \pm 29$                  | 4160  |
| 0645+74 Mrk 6       | $384 \pm 8$                   | 5775  |
| 0737+35 Mrk 78      | <sup>c</sup>                  | <sup>c</sup>  |
| 0921+52 Mrk 110     | $288 \pm 5$                   | 10560   |
| 0943-14 NGC 2992    | $131 \pm 5$                   | 2370  |
| 0945+50 Mrk 124     | $403 \pm 59$                  | 17005   |
| 1020+20 NGC 3227    | $514 \pm 6$                   | 1120  |
| 1103+72 NGC 3516    | $248 \pm 5$                   | 2650  |
| 1208+39 NGC 4151    | $343 \pm 6$                   | 950   |
| 1336+48 Mrk 266a    | $390 \pm 24$                  | 8386  |
| Mrk 266b            | $315 \pm 38$                  | 8230  |
| 1339+67 Mrk 270     | $358 \pm 9$                   | 3094  |
| 1415+25 NGC 5548    | $396 \pm 7$                   | 5060  |
| 1612+26 Ton 256     | $392 \pm 20$                  | 39300   |
| 1939-10 NGC 6814    | $129 \pm 6$                   | 1630  |
| 2041-10 Mrk 509     | $526 \pm 26$                  | 10375   |
| 2130+09 II Zw 136   | $349 \pm 7$                   | 18910   |
| 2221-02 3C 445      | $213 \pm 9$                   | 16890   |
| 2251-17 MR          | $563 \pm 13$                  | 19285   |
| 2300+08 NGC 7469    | $334 \pm 8$                   | 4830  |
| 2302-08 MCG 2-58-22 | $358 \pm 6$                   | 14045   |

<sup>a</sup> Estimated error:  $\pm 20 \text{ km s}^{-1}$ .

<sup>b</sup> Line wide and uneven; both baseline and peak position ill-determined.

<sup>c</sup> Double-peak profile.

red side of the peak): this is true for 20 of the 25 objects in this sample. If the intrinsic distribution in C20/W50 were symmetric about zero, the probability of selecting a sample of 25 objects of which only five or fewer are in either the positive or negative category (two-tailed test) is  $2 \times 10^{-4}$ . This asymmetric distribution has been noted also by HMVB and by Heckman, Miley, and Green (1984). The evidence for the reality of this effect is quite strong.

#### c) Is There Any Relationship between [O III] Emission-Line Characteristics and Other Seyfert Properties?

The present sample of objects is diverse in a number of observable characteristics: the nonthermal luminosities range over more than three orders of magnitude; the objects are spectroscopically diverse (all types of Seyfert are represented); and the host galaxies are “geometrically” varied, covering a broad range in axial ratio.

The following specific possible correlations were examined:

1. Is there a relationship between [O III] line profile properties and indicators of nonthermal nuclear luminosity? This question can be addressed only for intermediate or type 1 Seyferts and other broad-line objects, where such luminosity indicators exist (2–10 keV X-ray and broad-line H $\beta$  luminosities were examined here); no good indicators exist for Seyfert 2 objects.

TABLE 3  
DIMENSIONLESS MEASURES OF [O III] LINE PROFILE SHAPE

| Object       | W80/W50 | ±     | W20/W50 | ±     | C80/W50 | ±     | C50/W50 | ±     | C20/W50 | ±     | CB/W50 | ±    | CR/W50 | ±    |
|--------------|---------|-------|---------|-------|---------|-------|---------|-------|---------|-------|--------|------|--------|------|
| III Zw 2     | 0.466   | 0.018 | 1.583   | 0.032 | -0.010  | 0.010 | -0.062  | 0.010 | -0.121  | 0.010 | 0.85   | 0.08 | 0.66   | 0.04 |
| PG 0026 + 12 | 0.421   | 0.024 | 1.915   | 0.099 | 0.000   | 0.012 | 0.000   | 0.012 | 0.049   | 0.025 | 0.52   | 0.07 | 0.52   | 0.06 |
| Mrk 1        | 0.365   | 0.026 | 1.906   | 0.109 | 0.033   | 0.008 | -0.040  | 0.023 | -0.152  | 0.019 | 0.36   | 0.10 | 0.22   | 0.04 |
| NGC 526A     | 0.290   | 0.025 | 1.476   | 0.071 | 0.043   | 0.014 | -0.143  | 0.015 | -0.219  | 0.034 |        |      |        |      |
| Mrk 590      | 0.290   | 0.030 | 1.688   | 0.015 | 0.010   | 0.010 | 0.008   | 0.024 | -0.076  |       |        |      |        |      |
| AKN 79       | 0.455   | 0.083 |         |       | -0.127  | 0.031 | -0.153  | 0.042 |         |       |        |      |        |      |
| Mrk 1040     | 0.490   | 0.034 | 1.553   | 0.091 | 0.059   | 0.010 | 0.013   | 0.013 | -0.059  | 0.030 | 0.80   | 0.30 | 0.12   | 0.02 |
| NGC 1068     |         |       |         |       |         |       |         |       |         |       |        |      |        |      |
| NGC 1275     |         |       |         |       |         |       |         |       |         |       |        |      |        |      |
| 1E 0412-08   | 0.513   | 0.035 | 2.119   | 0.115 | 0.081   | 0.019 | 0.081   | 0.019 | 0.181   | 0.026 | 0.67   | 0.02 | 0.49   | 0.02 |
| 3C 120       | 0.511   | 0.039 | 1.426   | 0.170 | -0.015  | 0.011 | -0.056  | 0.015 | 0.030   | 0.053 | 0.23   | 0.06 | 0.70   | 0.19 |
| Mrk 3        | 0.567   | 0.029 | 1.539   | 0.058 | -0.001  | 0.010 | -0.074  | 0.015 | -0.184  | 0.015 |        |      |        |      |
| Mrk 6        | 0.362   | 0.017 | 2.917   | 0.255 | 0.000   | 0.008 | -0.102  | 0.008 | -0.313  | 0.063 |        |      |        |      |
| Mrk 78       |         |       |         |       |         |       |         |       |         |       |        |      |        |      |
| Mrk 110      | 0.618   | 0.020 | 1.594   | 0.085 | 0.014   | 0.011 | 0.000   | 0.010 | -0.038  | 0.014 | 0.31   | 0.08 | 0.34   | 0.05 |
| NGC 2992     | 0.405   | 0.041 | 2.740   | 0.238 | 0.031   | 0.023 | -0.008  | 0.024 | -0.412  | 0.070 | 1.96   | 0.18 | 0.53   | 0.03 |
| Mrk 124      | 0.347   | 0.118 |         |       | -0.005  | 0.053 | -0.069  | 0.018 |         |       |        |      |        |      |
| NGC 3227     | 0.500   | 0.011 | 1.638   | 0.052 | -0.097  | 0.006 | -0.193  | 0.008 | -0.212  | 0.016 | 0.25   | 0.02 | 0.51   | 0.03 |
| NGC 3516     | 0.504   | 0.023 | 2.173   | 0.114 | 0.012   | 0.012 | 0.012   | 0.012 | -0.161  | 0.016 | 0.57   | 0.04 | 0.49   | 0.04 |
| NGC 4151     | 0.315   | 0.016 | 1.770   | 0.041 | 0.020   | 0.009 | -0.149  | 0.012 | -0.198  | 0.012 | 0.53   | 0.02 | 0.66   | 0.02 |
| Mrk 266a     | 0.392   | 0.064 | 2.185   | 0.336 | -0.028  | 0.026 | -0.018  | 0.026 | -0.179  | 0.075 |        |      |        |      |
| Mrk 266b     | 0.314   | 0.041 | 1.848   | 0.237 | -0.022  | 0.010 | 0.114   | 0.062 | -0.032  | 0.029 | 0.32   | 0.12 | 0.38   | 0.14 |
| Mrk 270      | 0.279   | 0.016 | 1.581   | 0.069 | -0.011  | 0.008 | 0.115   | 0.012 | 0.151   | 0.020 | 0.36   | 0.03 | 0.26   | 0.03 |
| NGC 5548     | 0.497   | 0.018 | 1.793   | 0.066 | -0.018  | 0.008 | -0.061  | 0.008 | -0.126  | 0.013 | 0.30   | 0.03 | 0.47   | 0.05 |
| Ton 256      | 0.561   | 0.031 | 1.587   | 0.110 | -0.051  | 0.008 | -0.176  | 0.025 | -0.265  | 0.019 | 0.65   | 0.13 | 0.35   | 0.06 |
| NGC 6814     | 0.496   | 0.045 | 2.426   | 0.129 | 0.047   | 0.024 | 0.000   | 0.023 | -0.240  | 0.033 | 0.86   | 0.06 | 0.58   | 0.03 |
| Mrk 509      | 0.658   | 0.035 | 1.479   | 0.164 | 0.032   | 0.008 | -0.017  | 0.019 | -0.055  | 0.040 | 0.56   | 0.18 | 0.31   | 0.07 |
| II Zw 136    | 0.441   | 0.017 | 2.063   | 0.398 | 0.029   | 0.009 | -0.020  | 0.009 | -0.330  | 0.124 |        |      |        |      |
| 3C 445       | 0.465   | 0.031 | 1.808   | 0.128 | -0.005  | 0.015 | -0.038  | 0.019 | -0.136  | 0.029 | 0.41   | 0.08 | 0.26   | 0.08 |
| MR 2251-17   |         |       |         |       |         |       |         |       |         |       |        |      |        |      |
| NGC 7469     | 0.467   | 0.021 | 1.763   | 0.105 | 0.003   | 0.009 | -0.057  | 0.009 | -0.216  | 0.036 | 0.73   | 0.09 | 0.24   | 0.02 |
| MCG 2-58-22  | 0.374   | 0.015 | 1.838   | 0.049 | -0.003  | 0.009 | 0.095   | 0.009 | 0.277   | 0.026 |        |      |        |      |
| Mean         | 0.45    |       | 1.78    | 0.00  | 0.00    |       | -0.03   |       | -0.09   |       | 0.51   |      | 0.41   |      |
| Sigma        | 0.10    |       | 0.27    | 0.045 | 0.045   |       | 0.08    |       | 0.15    |       | 0.22   |      | 0.16   |      |

NOTE.—Lacunae in the table indicate cases where the defined quantities cannot be determined in a stable fashion or are not meaningful. In particular, (1) The 20% level measures for Mrk 590 were determined by hand due to baseline glitches. (2) NGC 1068 and NGC 1275 have [O III] profiles which are so wide that a baseline cannot be determined properly. (3) Mrk 78 has a double-peaked profile; the usual measures are not applicable. (4) The profile of MR 2251-17 is very irregular; the usual measures are not meaningful. (5) Other gaps indicate very large estimated errors.

TABLE 4  
CONVERSION OF LINE PROFILE MEASURES

| Measures from Other Works <sup>a</sup> |   | Equivalent Measures in This Work |
|--|---|----------------------------------|
| W50                                    | ↔ | W50                              |
| W80/W50                                | ↔ | W80/W50                          |
| $R_{20/50}$                            | ↔ | W20/W50                          |
| C80/W50                                | ↔ | C80/W50 - C50/W50                |
| C20/W50                                | ↔ | C20/W50 - C50/W50                |
| A120                                   | ↔ | $2(C80/W50 - C20/W50)/(W20/W50)$ |

<sup>a</sup> As defined by Heckman *et al.* 1981 and Heckman, Miley, and Green 1984.

2. Are the line profile measures related to the axial ratios of the host galaxies? Published axial ratio estimates are available for 22 of the objects studied here (Keel 1980; Su and Simkin 1980; Lawrence and Elvis 1982); they range from 0.17 to 0.93, but the values are highly uncertain, as indicated by substantial discrepancies among these sources.

3. Can a relation be found between properties of the broad-line regions and the characteristics of the [O III] lines? Two potential indicators of broad-line region structure were examined: the FWZI of H $\alpha$  and the H $\alpha$ /H $\beta$  luminosity ratio.

4. Is there any difference in the distributions of [O III] line measures of objects of different type or class? (The classifications of the sources are shown in Table 1).

5. Do any of the line profile properties correlate with the galaxy colors? (The  $B-V$  colors do, in general, correlate well with nonthermal luminosity, since nuclei whose optical emission is dominated by the central source continuum are bluer than those dominated by starlight.)

On the basis of the present data, *no* significant correlations or differences have been found in any of the above categories. This is in general agreement with previous work except on point (3); based on a larger number of objects than available in this work, Heckman, Miley, and Green (1984) have claimed that there is a correlation between [O III] W50 and both FWHM and FWZI of broad-line H $\alpha$ . Should future work confirm this, the implications for connections between the narrow- and broad-line regions may prove interesting.

Some questions of possible interest have not been considered because the present data are not especially informative: (1) HMVB have found an interesting correlation (in a sample of 11 objects) between the *narrow* H $\alpha$ /H $\beta$  ratio (indicative of NLR obscuration) and the [O III] line asymmetry. Unfortunately, objects with well-determined narrow Balmer-line ratios are underrepresented in the current work; the five objects available do show a trend in the expected direction (large H $\alpha$ /H $\beta$  associated with large [negative C20/W50] asymmetry), but no conclusion can be formulated from a sample of this size. (2) It has been claimed (Wilson and Willis 1980; HMVB) that [O III] line widths are strongly correlated with ratio power from the steep-spectrum sources of  $\sim 1$  kpc size (but not with the radio power from the more compact flat-spectrum sources). The question has been reexamined using the line widths obtained in this work; nine objects have both measured steep-spectrum radio sources and well-defined line widths. There is a weak trend in the direction of the suggested correlation, but this is dominated by a single object of large line width and high radio power (Mrk 3). On the basis of the present measurements, this possibility can be neither supported nor rejected.

#### IV. COMPARISON OF GALAXIAN SYSTEM AND [O III] VELOCITIES

The relationship in velocity between the central nonthermal sources of the galaxies and the emission-line profiles may be of considerable interest for the understanding of the emitting regions. Unfortunately, the nonthermal source velocities are inaccessible, and even the broad-line region velocities can be only very inaccurately determined because the broad-line peaks are so ill-defined. The best that can be done is to determine effective velocities for the galaxies.

There are several ways of determining this "system" velocity. To date, this has been attempted mainly by means of 21 cm H I observations (e.g., Heckman, Balick, and Sullivan 1978), but this method has several drawbacks: (1) Some galaxies are weak 21 cm emitters, and the technique cannot be applied at all. (2) Some galaxies (e.g., Mrk 3 and NGC 7469) are in interacting systems, which makes the results very suspect. (3) Occasionally strong emission from a noninteracting galaxy is detected, but the line profile is so broad or irregular that it is very difficult to assign a central velocity with any substantial accuracy.

Another approach to determining the system velocities of galaxies is through measurement of the velocities of the stellar absorption lines. This has the difficulty that for sources strongly dominated by nonthermal radiation the absorption lines may be too weak to detect. However, we have obtained low-dispersion spectra suitable for absorption-line measurement for 22 of the 32 objects presented in this work. The spectra were taken at the Whipple Observatory 1.5 m telescope at a resolution of 150–300 km s<sup>-1</sup>; reduction and analysis follow the techniques of the Center for Astrophysics redshift program (Tonry 1980; Tonry and Davis 1979), in which velocities are determined by cross-correlation with a template spectrum of well-known velocity. (All velocities used here are defined as *cz* and are corrected to a heliocentric frame.) Absorption-line velocities from spectra for seven of the 22 observed galaxies were rejected for unreliable or low-quality cross correlation.

An estimate of the error in this process based on internal information alone may overlook important systematic errors. In particular, systematic positioning of the spectrograph slit away from the center of a galaxy along the direction of the apparent major axis may result in substantial velocity errors. A typical rotation curve of a spiral galaxy (see, e.g., Mihalas and Binney 1981) rises linearly from zero at the galactic nucleus to  $\sim 250$  km s<sup>-1</sup> at a distance of  $\sim 1.5$  kpc before flattening out. Hence, for a small slit mispositioning by angle  $\delta$  (arcsec) on the sky, we may expect a velocity error  $\Delta v = 8.1 \times 10^{-3}(\delta)(cz)(h^{-1})$  km s<sup>-1</sup>, where  $h = H_0/100$  km s<sup>-1</sup> Mpc<sup>-1</sup>. This could result in a velocity error of several tens of kilometers per second for a typical galaxy in this sample. Similar difficulties may be produced by spectrograph misalignments which cause light from the telescope to follow a slightly different path than light from the comparison lamp. Several approaches have been taken to check the data for this kind of problem.

First, the internal consistency of the absorption-line results is checked in those cases where more than one spectrum is available for a given source. Table 5 exhibits the six individual cases and the deviations from the mean (normalized to the formal error) of these cases. The distribution of these deviations has a dispersion  $\sigma = 0.8$ , indicating that the formal errors may be somewhat larger than  $1 \sigma$ . The various spectra of a given object were taken substantially apart in time, from days

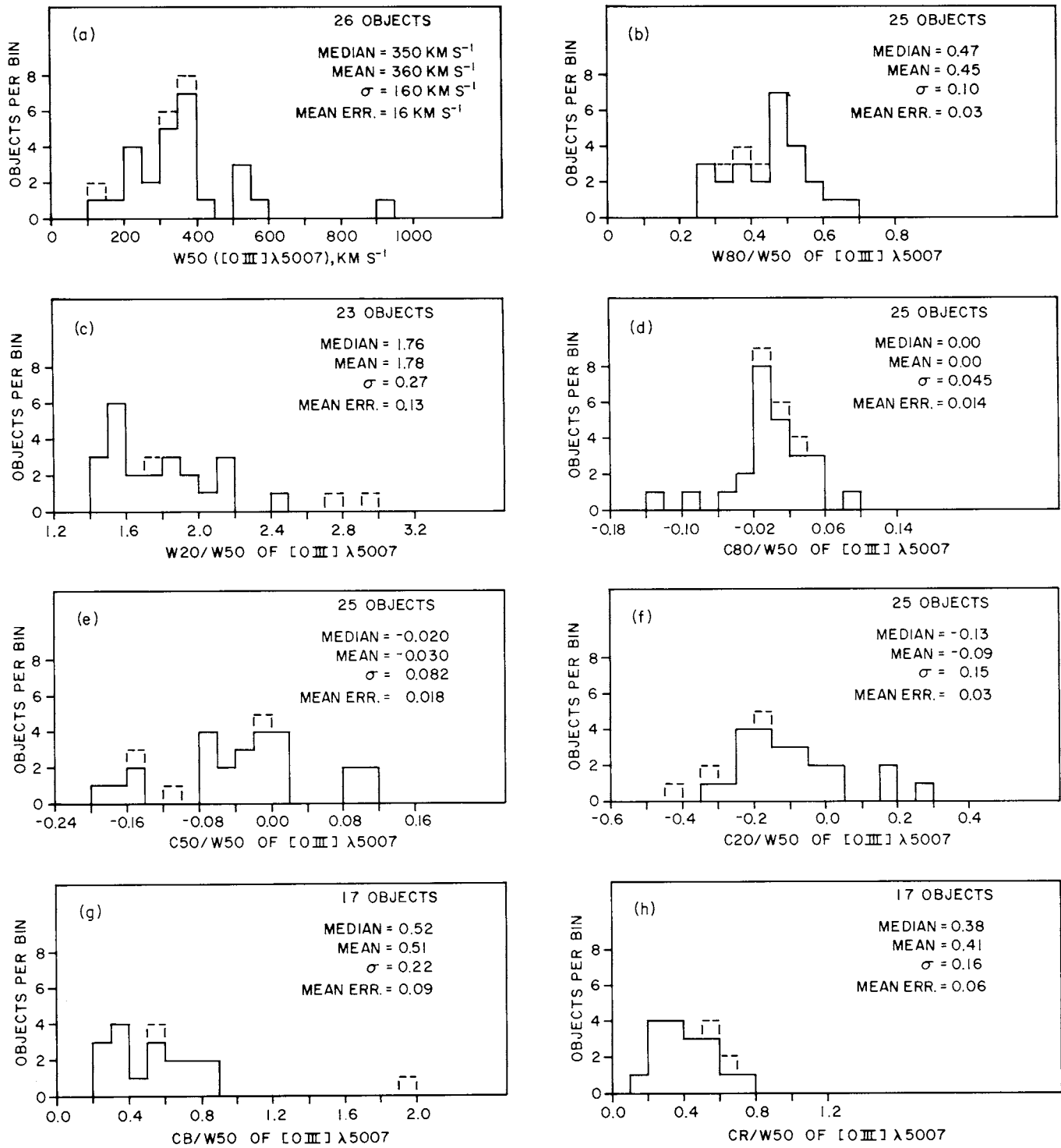


FIG. 7.—Histograms showing the distributions of the data in the line profile measures. The mean, median, and dispersion of each measure are shown, as well as the number of objects on which these values are based and the mean assigned error for those objects. Mrk 6, NGC 2992, and NGC 4151 are shown as dashed extensions to the histograms (and are not included in the calculated mean, median, etc.) since the current measurements have probably significantly undersampled the emitting regions in these objects. (a) W50; (b) W80/W50; (c) W20/W50; (d) C80/W50; (e) C50/W50; (f) C20/W50; (g) CB/W50; (h) CR/W50.

TABLE 5  
INTERNAL CONSISTENCY OF ABSORPTION-LINE VELOCITIES  
FROM SEVERAL SPECTRA OF SAME SOURCE

| Object         | Velocity                                  | Weighted Mean                 | $(v - v_{\text{mean}})/\Delta v$ |
|----------------|---|-------------------------------|----------------------------------|
|                | $v \pm \Delta v$<br>(km s <sup>-1</sup> ) | Velocity<br>$v_{\text{mean}}$ |                                  |
| Mrk 590 .....  | 7891 ± 21                                 | 7911                          | -0.95                            |
|                | 7925 ± 18                                 |                               | 0.78                             |
| AKN 79 .....   | 5241 ± 24                                 | 5235                          | 0.25                             |
|                | 5231 ± 15                                 |                               | -0.27                            |
| NGC 1068 ..... | 1134 ± 18                                 | 1151                          | -0.94                            |
|                | 1139 ± 20                                 |                               | -0.60                            |
|                | 1155 ± 23                                 |                               | 0.17                             |
|                | 1164 ± 13                                 |                               | 1.00                             |
| NGC 2992 ..... | 2360 ± 22                                 | 2328                          | 1.45                             |
|                | 2325 ± 25                                 |                               | -0.20                            |
|                | 2292 ± 25                                 |                               | -1.44                            |
| NGC 3516 ..... | 2658 ± 23                                 | 2649                          | 0.39                             |
|                | 2631 ± 33                                 |                               | -0.55                            |
| NGC 4151 ..... | 1005 ± 26                                 | 1014                          | -0.35                            |
|                | 1018 ± 16                                 |                               | 0.25                             |

to years, which indicates that the technique gives very stable results.

Table 6 compares our absorption-line velocities with 21 cm velocities of Heckman, Balick, and Sullivan (1978) for the four objects in common. Errors of 20 km s<sup>-1</sup> are adopted for the latter, as suggested by Heckman *et al.* for their “good” profiles. Three of the four differences in the table are within one error bar of zero; this is consistent with correct assignment of error bar sizes in both of the techniques under comparison. Since one technique detects the stellar component whereas the other technique detects the gaseous component of a galaxy, this comparison not only tests the accuracy (i.e., freedom from systematic error) of each technique, but also supports the view that there indeed exists an effective “system” velocity which is correctly measured by both techniques independently.

The assignment of errors in the system velocities in this work is also supported by the extensive experience of the Center for Astrophysics redshift program; the mean error of 24 km s<sup>-1</sup> in our system velocity results is consistent for spectra of this quality, both with the early evaluation of the errors (Tonry and Davis 1979) and with the continuing experience of the program (Huchra 1983).

The above paragraphs indicate that we can reliably determine (and estimate the errors in) system velocities. We now

TABLE 6  
CONSISTENCY OF ABSORPTION-LINE VELOCITIES  
WITH 21 CENTIMETER VELOCITIES

| Object         | Absorption-Line<br>Velocity <sup>a</sup><br>(km s <sup>-1</sup> ) | 21 cm<br>Velocity <sup>b</sup><br>(km s <sup>-1</sup> ) | Velocity<br>Difference <sup>c</sup> |
|----------------|---|---|-------------------------------------|
| NGC 1068 ..... | 1151 ± 13   | 1140 ± 20   | 11 ± 24                             |
| NGC 3227 ..... | 1145 ± 28   | 1106 ± 20   | 39 ± 34                             |
| NGC 4151 ..... | 1014 ± 16   | 994 ± 20  | 20 ± 26                             |
| NGC 6814 ..... | 1544 ± 24   | 1560 ± 20   | -16 ± 31                            |

<sup>a</sup> From this work.

<sup>b</sup> From Heckman, Balick, and Sullivan 1978.

<sup>c</sup> Col. (2) minus col. (3).

TABLE 7  
CONSISTENCY OF [O III] EMISSION-LINE VELOCITIES FROM TWO SOURCES

| OBJECT         | C50 VELOCITY                       |   | VELOCITY<br>DIFFERENCE <sup>a</sup><br>(km s <sup>-1</sup> ) |
|----------------|------------------------------------|---|--|
|                | This Work<br>(km s <sup>-1</sup> ) | Heckman <i>et al.</i> 1981<br>(km s <sup>-1</sup> ) |  |
| Mrk 3 .....    | 4093 ± 14                          | 4050 ± 30   | 43 ± 33  |
| Mrk 6 .....    | 5736 ± 5                           | 5680 ± 30   | 56 ± 30  |
| NGC 2992 ..... | 2369 ± 5                           | 2375 ± 30   | -6 ± 30  |
| NGC 4151 ..... | 899 ± 5                            | 905 ± 30  | -6 ± 30  |
| Mrk 270 .....  | 3135 ± 6                           | 3125 ± 30   | 10 ± 31  |
| NGC 5548 ..... | 5036 ± 5                           | 5030 ± 30   | 6 ± 30   |
| NGC 7469 ..... | 4811 ± 5                           | 4790 ± 30   | 21 ± 30  |

<sup>a</sup> Col. (2) minus col. (3).

examine the other component of the difference velocity in which we are interested, namely, the velocities of the [O III]  $\lambda 5007$  emission lines. There is no opportunity here for internal checks in our data (nor is it so important to have such checks, since the random errors in these high-resolution spectra are very low), but we can compare our results for seven objects with published values from HMVB as a check primarily against systematic errors (see Table 7). For five of seven examples, the difference in velocity between this and previous work lies within the indicated errors, which supports the view that the errors have been correctly assigned at  $\sim 1 \sigma$ . The velocities used here are those of the line centers measured at the 50% level; these are very well determined and allow direct comparison with the result of HMVB.

We have shown that there are no evident discrepancies internal to our data or between this work and previous, both in the emission-line and in the system velocities. We have found both emission-line and system velocities for 13 objects; these are shown in Table 8 along with their differences. (Positive values indicate a line peak that is redshifted with respect to the system center-of-mass velocity.) The mean error in the 13 differences is 26 km s<sup>-1</sup>. The distribution of results (Fig. 8) has a mean of 16.5 km s<sup>-1</sup> and a  $1 \sigma$  dispersion of 84.0 km s<sup>-1</sup>; this distribution is consistent with symmetry about zero. Figure 8 also shows the earlier work of HMVB. The two distributions clearly differ significantly: a two-tailed Smirnov two-sample test rejects with greater than 99% confidence the hypothesis that they were drawn from the same parent distribution.

It is not clear, given the consistency tests between the velocities which have been shown above, why the results from this work are inconsistent with the results of HMVB. It is possible that there are measurement errors in objects other than the few where checks have been possible or that the small number of objects in the samples is responsible for the difference. We shall return to this topic in Paper II in connection with kinematic models of the NLRs.

The velocity differences from the present work have been examined for any correlations with line asymmetry measures, source luminosity, redshift (i.e., projected slit size), galaxy axial ratio, and source type; none were found.

## V. CONCLUSIONS

Our work makes available a body of spectra of active galactic nuclei in the bright [O III]  $\lambda 5007$  emission line; the observations are of sufficient resolution and signal-to-noise to provide information on narrow-line region kinematics. The line profiles have been described in a way which facilitates the study of their

TABLE 8  
COMPARISON OF EMISSION-LINE AND SYSTEM VELOCITIES

| Object              | Adopted Heliocentric Velocity ( $cz$ ) of System ( $\text{km s}^{-1}$ ) | C50 Velocity ( $cz$ ) of [O III] $\lambda 5007$ ( $\text{km s}^{-1}$ ) | $V(\text{C50}) - V(\text{Sys})$ ( $\text{km s}^{-1}$ ) |
|---------------------|---|--|--|
| 0008+10 III Zw 2    | ...   | $26831 \pm 5$  | ...  |
| 0026+12 PG          | ...   | $43565 \pm 5$  | ...  |
| 0113+32 Mrk 1       | ...   | $4799 \pm 13$  | ...  |
| 0121-35 NGC 526A    | $5710 \pm 34$   | $5710 \pm 5$   | $0 \pm 34$   |
| 0212-01 Mrk 590     | $7911 \pm 18$   | $7893 \pm 10$  | $-18 \pm 21$   |
| 0214+38 AKN 79      | $5235 \pm 15$   | $5316 \pm 15$  | $81 \pm 21$  |
| 0225+31 Mrk 1040    | $4889 \pm 38$   | $4949 \pm 5$   | $60 \pm 38$  |
| 0240-00 NGC 1068    | $1151 \pm 13$   | ...  | ...  |
| 0316+41 NGC 1275    | ...   | ...  | ...  |
| 0412-08 1E          | ...   | $11468 \pm 5$  | ...  |
| 0430+05 3C 120      | ...   | $9905 \pm 6$   | ...  |
| 0609+71 Mrk 3       | $4015 \pm 34$   | $4093 \pm 14$  | $78 \pm 37$  |
| 0645+74 Mrk 6       | $5553 \pm 33$   | $5736 \pm 5$   | $183 \pm 33$   |
| 0737+65 Mrk 78      | $11090 \pm 24$  | ...  | ...  |
| 0921+52 Mrk 110     | ...   | $10560 \pm 5$  | ...  |
| 0943-14 NGC 2992    | $2328 \pm 22$   | $2369 \pm 5$   | $41 \pm 23$  |
| 0945+50 Mrk 124     | ...   | $16977 \pm 7$  | ...  |
| 1020+20 NGC 3227    | $1145 \pm 28$   | $1021 \pm 5$   | $-124 \pm 28$  |
| 1103+72 NGC 3516    | $2649 \pm 23$   | $2653 \pm 5$   | $4 \pm 24$   |
| 1208+39 NGC 4151    | $1014 \pm 16$   | $899 \pm 5$  | $-115 \pm 17$  |
| 1336+48 Mrk 266a    | ...   | $8379 \pm 11$  | ...  |
| Mrk 266b            | ...   | $8266 \pm 20$  | ...  |
| 1339+67 Mrk 270     | $3147 \pm 15$   | $3135 \pm 6$   | $-12 \pm 16$   |
| 1415+25 NGC 5548    | ...   | $5036 \pm 5$   | ...  |
| 1612+26 Ton 256     | ...   | $39231 \pm 9$  | ...  |
| 1939-10 NGC 6814    | $1552 \pm 24$   | $1630 \pm 5$   | $78 \pm 25$  |
| 2041-10 Mrk 509     | ...   | $10366 \pm 11$   | ...  |
| 2130+09 II Zw 136   | ...   | $18903 \pm 5$  | ...  |
| 2221-02 3C 445      | ...   | $16882 \pm 5$  | ...  |
| 2251-17 MR          | ...   | $19137 \pm 6$  | ...  |
| 2300+08 NGC 7469    | $4852 \pm 19$   | $4811 \pm 5$   | $-41 \pm 20$   |
| 2302-08 MCG 2-58-22 | ...   | $14079 \pm 5$  | ...  |

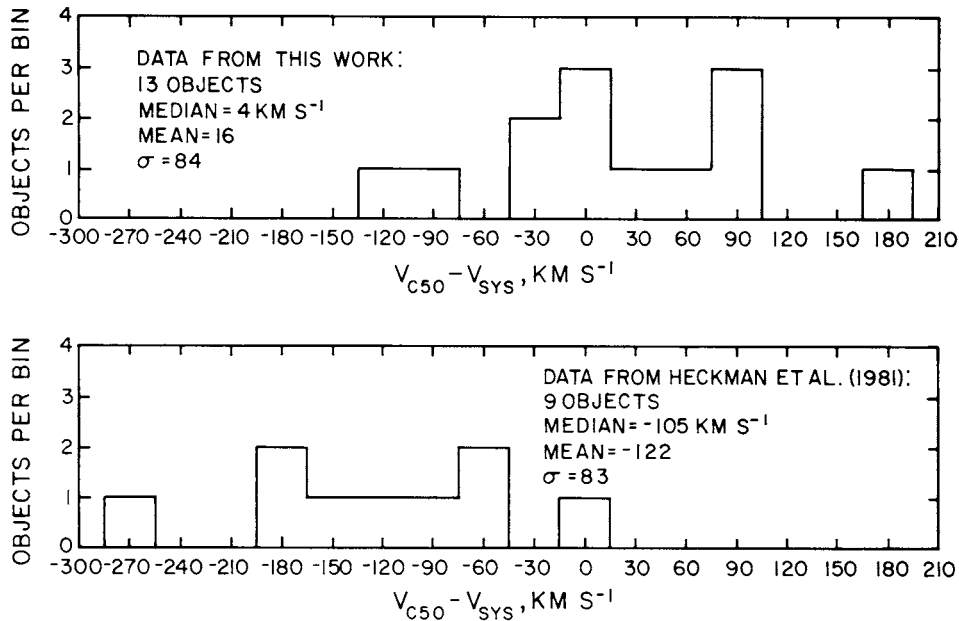


FIG. 8.—Distribution of differences between [O III] line center at half-maximum  $V_{\text{C50}}$  and system velocity  $V_{\text{sys}}$ , as determined in this work (13 objects) and as reported by Heckman *et al.* (1981) for nine objects.

properties, the search for relationships with other properties of the sources, and ultimately their comparison with models. In particular, the distributions of profile properties are presented; the most significant result here is the predominance of line profiles which fall off more slowly to the blue than to the red side of the peak, confirming a trend noted earlier. The distribution of emission-line velocities with respect to the "system" velocities of the host galaxies has been investigated; the results, symmetric about zero difference velocity, differ from previous work. The interpretation of these points will be deferred to Paper II since their meaning is substantially clarified by reference to a collection of kinematic models.

There are few if any correlations involving the [O III] line profiles which argue for a particular kinematic or geometric picture of the NLR, and the line profiles themselves cannot be directly interpreted in kinematic terms. This confirms the need for an interpretive tool for the present data, such as can be

provided by a simple group of kinematic models. Paper II describes a way in which such a comparison can be carried through with reference to a particular class of models; however, the data are presented here in a form which should permit easy comparison with any model which may be developed in the course of future work.

The authors would like to acknowledge extensive discussions with and many useful suggestions from Drs. A. Cameron, M. Geller, L. Hartmann, J. Huchra, J. Krolik, and W. Traub. Drs. F. Chaffee, J. Huchra, and D. Latham were instrumental in obtaining some of the spectra essential to this work. We would also like to thank the staffs of the Multiple Mirror Telescope and of the Whipple Observatory for assistance in obtaining the data. One of us (J.V.) has been supported by a NAS/NRC Research Associateship during part of the preparation of this paper.

## REFERENCES

- Burbidge, G., and Crowne, A. H. 1979, *Ap. J. Suppl.*, **40**, 583.  
 Burbidge, G. R., Crowne, A. H., and Smith, H. E. 1977, *Ap. J. Suppl.*, **33**, 113.  
 Chaffee, F. H., and Latham, D. W. 1982, *Pub. A.S.P.*, **94**, 386.  
 Clements, E. D. 1981, *M.N.R.A.S.*, **197**, 829.  
 Davidson, K., and Netzer, H. 1979, *Rev. Mod. Phys.*, **51**, 715.  
 Davis, M., and Latham, D. 1979, *Proc. SPIE*, **172**, 71.  
 Feldman, F. R., Weedman, D. W., Balzano, V. A., and Ramsey, L. W. 1982, *Ap. J.*, **256**, 427.  
 Ferland, G. J., and Mushotzky, R. F. 1982, *Ap. J.*, **262**, 564.  
 Gallouet, N., Heidmann, N., and Dampierre, F. 1975, *Astr. Ap. Suppl.*, **19**, 1.  
 Halpern, J. P. 1982, Ph.D. thesis, Harvard University.  
 Heckman, T. M., Balick, B., and Sullivan, W. T. 1978, *Ap. J.*, **224**, 745.  
 Heckman, T. M., Miley, G. K., and Green, R. F. 1984, *Ap. J.*, **281**, 525.  
 Heckman, T. M., Miley, G. K., van Breugel, W. J. M., and Butcher, H. R. 1981, *Ap. J.*, **247**, 403 (HMVB).  
 Hewitt, A., and Burbidge, G. 1980, *Ap. J. Suppl.*, **43**, 57.  
 Huchra, J. P. 1983, private communication.  
 Keel, W. C. 1980, *A.J.*, **85**, 198.  
 Kojoian, G., Elliott, R., and Tovmassian, H. M. 1978, *A.J.*, **83**, 1545.  
 Krolik, J. H., McKee, C. F., and Tarter, C. B. 1981, *Ap. J.*, **249**, 422.  
 Krolik, J. H., and Vrtilek, J. M. 1984, *Ap. J.*, **279**, 521.  
 Kwan, J., and Krolik, J. H. 1981, *Ap. J.*, **250**, 478.  
 Latham, D. W. 1982, in *IAU Colloquium 67, Instrumentation for Astronomy with Large Optical Telescopes*, ed. C. M. Humphries (Dordrecht: Reidel), p. 259.  
 Lawrence, A., and Elvis, M. 1982, *Ap. J.*, **256**, 410.  
 Markarian, B. E., Lipovetskii, V. A., and Stepanyan, D. A. 1977, *Astrofizika*, **13**, 397.  
 Mihalas, D., and Binney, J. 1981, *Galactic Astronomy: Structure and Kinematics* (San Francisco: Freeman).  
 Mushotzky, R. F. 1982, *Ap. J.*, **256**, 92.  
 Nieto, J.-L. 1978, *A.J.*, **83**, 1141.  
 Osterbrock, D. E. 1977, *Ap. J.*, **215**, 733.  
 Osterbrock, D. E., and Koski, A. T. 1976, *M.N.R.A.S.*, **176**, 61P.  
 Pelat, D., Alloin, D., and Fosbury, R. 1981, *M.N.R.A.S.*, **195**, 787.  
 Peterson, S. D. 1973, *A.J.*, **78**, 811.  
 Petrosian, A. R. 1980, *Astrofizika*, **16**, 631.  
 Petrosian, A. R., Saakyan, K. A., and Khachikyan, E. E. 1980, *Astrofizika*, **16**, 621.  
 Phillips, M. M. 1980, *Ap. J. (Letters)*, **236**, L45.  
 Phillips, M. M., Baldwin, J. A., Atwood, B., and Carswell, R. F. 1983, *Ap. J.*, **274**, 558.  
 Puetter, R. C., Smith, H. E., Willner, S. P., and Pipher, J. L. 1981, *Ap. J.*, **243**, 345.  
 Steiner, J. E. 1981, *Ap. J.*, **250**, 469.  
 Steiner, J. E., Grindlay, J. E., and Maccacaro, T. 1982, *Ap. J.*, **259**, 482.  
 Su, H. J., and Simkin, S. M. 1980, *Ap. J. (Letters)*, **238**, L1.  
 Tonry, J. L. 1980, Center for Astrophysics, Int. Memo.  
 Tonry, J., and Davis, M. 1979, *A.J.*, **84**, 1511.  
 Vrtilek, J. M. 1983, Ph.D. thesis, Harvard University.  
 ———. 1985, *Ap. J.*, **294**, 121 (Paper II).  
 Ward, M. J., Wilson, A. S., Penston, M. V., Elvis, M., Maccacaro, T., and Tritton, K. P. 1978, *Ap. J.*, **223**, 788.  
 Weedman, D. W. 1977, *Ann. Rev. Astr. Ap.*, **15**, 69.  
 Wilson, A. S., and Meurs, E. J. A. 1978, *Astr. Ap. Suppl.*, **33**, 407.  
 Wilson, A. S., and Willis, A. G. 1980, *Ap. J.*, **240**, 429.  
 Yee, H. K. C., and Oke, J. B. 1978, *Ap. J.*, **226**, 753.

N. P. CARLETON: Harvard-Smithsonian Center for Astrophysics, 60 Garden Street, Cambridge, MA 02138

J. M. VRTILEK: NASA/Goddard Institute for Space Studies, 2880 Broadway, New York, NY 10025